

The Determination of the Chemical Diffusion Coefficient of n-Type AgBr by Means of a D.c. Polarization Cell

Jun SASAKI,* Junichiro MIZUSAKI,* Shigeru YAMAUCHI, and Kazuo FUEKI

Department of Industrial Chemistry, Faculty of Engineering, The University of Tokyo,
Hongo, Bunkyo-ku, Tokyo 113

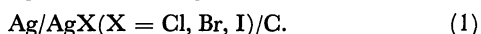
(Received December 23, 1980)

The electronic conductivity of AgBr and the chemical diffusion coefficient of n-type AgBr were measured by means of a d.c. polarization cell, \ominus Ag/AgBr/inert electrode \oplus , in the temperature range from 325 °C to 400 °C. In order to suppress the electrolysis of AgBr, a platinum plate was used instead of carbon as the inert anode. The chemical diffusion coefficient, \tilde{D} , was determined by two methods. One was the intermediate probe method (IP method) whereby the relaxation of the voltage between the Ag reversible electrode and the Pt intermediate probe, inserted into the middle of AgBr, was followed after an abrupt change in the polarization voltage. The other was the open-circuit method (OC method) whereby the terminal voltage of the cell was followed after the circuit of the cell had been opened. The electronic conductivity in the steady state was independent of the nature of the inert electrodes (Pt or C), provided that the inert electrode was completely sealed. However, it took more time for the cell with a carbon electrode to reach the steady state than that with a platinum one. The chemical diffusion coefficient, \tilde{D} , determined by the IP method for the Ag/AgBr/Pt cell agreed with that for the Ag/AgBr/C cell. The chemical diffusion coefficient, \tilde{D} , determined by the OC method for the Ag/AgBr/Pt cell agreed with that obtained by the IP method. The chemical diffusion coefficients determined by these methods were expressed by

$$\tilde{D} = 3.0 \times 10^8 \exp\left(\frac{-89.0 \text{ kJ mol}^{-1}}{RT}\right) / \text{cm}^2 \text{ s}^{-1}.$$

No chemical diffusion coefficient can be obtained by the OC method for the Ag/AgBr/C cell, because of the slow diffusion of the Br₂ gas produced by the electrolysis of AgBr from the carbon electrode.

Since the application of the d.c. polarization technique to the investigation of solid ionic conductors by Hebb¹⁾ and Wagner,²⁾ the method has been used widely to determine the electronic conductivities or chemical diffusion coefficients of halides of silver and copper.^{3–19)} Mizusaki *et al.*,^{7–10)} for instance, investigated silver halides by using the following cell:



Using the improved cell configuration shown in Fig. 1(a) (A-type cell), they found several important facts as follows:

(i) One can determine the chemical potential profile in AgX under d.c. polarization by measuring the voltage between the Ag electrode and the Pt probes inserted into AgX. The chemical potential profile obtained experimentally agrees with that expected from Wagner's theory.²⁾

(ii) In order to obtain the electronic conductivity,

the inert electrode (ion-blocking electrode) must be completely sealed.

(iii) The chemical diffusion coefficient, \tilde{D} , in AgX can be determined from the relaxation of the voltage between the Ag electrode and the Pt probe inserted into AgX after an abrupt change in the voltage applied to the cell.

The methods for the determination of the chemical diffusion coefficient by using the d.c. polarization cell^{6,9,11–17)} were classified as follows:

(i)^{6,11–15)} The method whereby the current is measured with the passage of time after the abrupt change in the polarization potential applied to the cell. (voltage step-transient current method; TC method).

(ii)⁹⁾ The method whereby the potential difference between the reversible (reference) electrode and the probe inserted into the sample is measured with the passage of time after a change in the polarization potential (voltage step-intermediate probe method; IP method).

(iii)^{16,17)} The method whereby the voltage of the cell is followed after the cell circuit has been opened (open circuit method; OC method).

Raleigh^{18,19)} measured the time change in the current by the TC method using the Ag/AgBr/Pt (or C) cell; he found that the current-time curve involved several time constants. The current was interpreted by the super-imposition of the current due to the charging of the double layer of the AgBr/Pt interface, the current due to the redistribution of electronic carriers within AgBr (chemical diffusion), and the electrolytic current of AgBr. It seems to be difficult, however, to measure these currents separately. Therefore, the TC method is not appropriate for determining the chemical diffusion coefficient.

The IP method has the advantage of measuring the

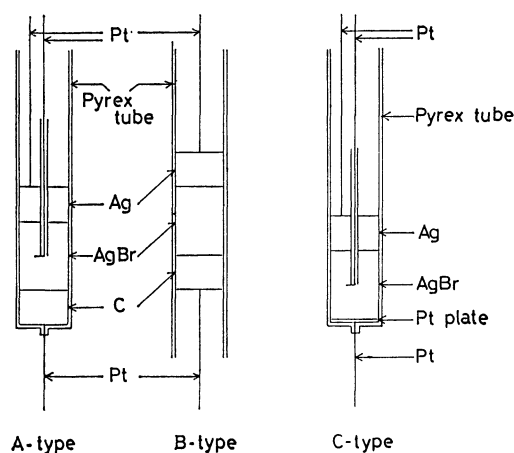


Fig. 1. Configurations of d.c. polarization cell.

change in the chemical potential profile directly. However, the influence of the electronic current flowing during the relaxation on the mass transfer caused by the chemical diffusion is not clear. From this point of view, the OC method is considered to be superior to the IP method, because the transient current does not flow during the chemical relaxation.

Weiss¹⁶⁾ determined \bar{D} in AgBr by means of the OC method using the cell shown in Fig. 1(b) (B-type cell). Since the carbon electrode was exposed to the inert atmosphere, it was doubtful that the decay of the open-circuit voltage gave the correct value of \bar{D} .⁹⁾ Even if an A-type cell is used, the Br₂ gas produced by the electrolysis of AgBr diffuses and is absorbed by the carbon electrode. Therefore, the decay of the open-circuit voltage may be supposed not to correspond to the chemical diffusion in AgBr because of the influence of the slow diffusion of Br₂ gas in the carbon electrode. In order to eliminate the influence of Br₂-gas diffusion in the carbon electrode, platinum should be used instead of carbon as follows:



Moreover, the cell configuration shown in Fig. 1(c) (C-type cell) should be used.

The present work aims to determine the electronic conductivity by the d.c. polarization method, and \bar{D} by means of the IP method and the OC method.

Experimental

Circuit and Measurement Procedure. Figure 2 shows a schematic diagram of the experimental circuit. The polarization voltage was applied by means of a potentiostat. The current was determined by measuring the IR drop which appeared between the two ends of a standard resistance, R_s , connected with the cell in series. The potential difference $E(X=L/2)$ between the Ag electrode and Pt probe inserted into AgBr and the open-circuit voltage were recorded by means of a voltage follower with high input impedance.

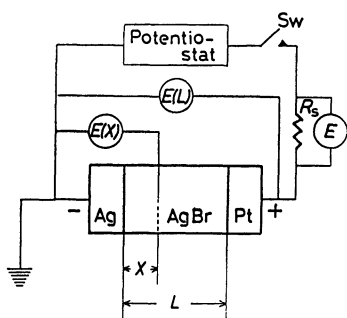


Fig. 2. Schematic diagram of experimental circuit.

IP Method: After the steady state under the applied voltage, E_1 , had been attained, a second voltage, E_2 , was suddenly applied to the cell by means of a function generator. The time changes in $E(X=L/2)$ and the current were recorded.

OC Method: After the steady state under the applied voltage, $E(L)$, has been attained, the circuit was opened and the time change in $E(L)$ was recorded.

The experiment was carried out in the temperature range from 325 to 400 °C. A polarization voltage below 300 mV

was applied. Under these experimental conditions, the electronic conduction of AgBr was of the n-type.

Samples and Cell Configurations. Rod-like single crystals of AgBr were prepared from the powder material of a 99.999% purity by means of the Bridgman method. The rod thus obtained was cut into disks 10 mm in diameter.

Figure 3 shows the construction of the cell. The surface of a platinum plate with platinum-lead wire was polished with 1 μm of alumina abrasive powder and then cleaned with an alkali cleaning solution. The platinum plate was then carefully sealed in a Pyrex tube so that no vacant spaces remained between the Pyrex tube and the platinum plate.

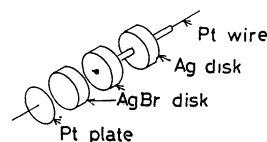


Fig. 3. Cell and samples.

Two AgBr disks of the same size were prepared. A hole 1.2 mm in diameter was drilled in the center of one AgBr disk for inserting the Pt probe. A platinum wire was insulated by means of a mullite tube 1.2 mm in diameter, its tip placed at the center of the interface of two AgBr disks. The surface of each AgBr disk was polished with 1 μm of alumina abrasive powder and cleaned by the use of an ultrasonic cleaner. The cell was constructed in a Pyrex tube 10 mm in inner diameter and was pressed with a slight pressure so that the side surface of the AgBr disk was assured of a good contact with the inside wall of the Pyrex tube as a result of the plastic deformation of AgBr at high temperatures. Thus, a good sealing of the ion-blocking electrode could be obtained.

In the present study, two types of cells, the A-type cell and the C-type cell shown in Fig. 1, were employed. The A-type cell was constructed in a way essentially similar to the C-type cell.

Results and Discussion

Electronic Conductivity. Under the steady state of d.c. polarization, the electronic current flowing in the cell (I) or (II) is represented by:^{2,8,10)}

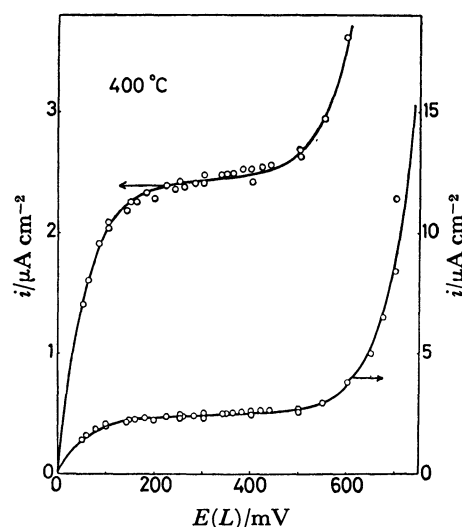


Fig. 4. Plot of i vs. $E(L)$ for C-type cell.

$$\frac{iFL}{RT} = \sigma_e^0 \left[1 - \exp\left(-\frac{E(L)F}{RT}\right) \right] + \sigma_h^0 \left[\exp\left(\frac{E(L)F}{RT}\right) - 1 \right], \quad (1)$$

where L is the thickness of the electrolyte, $E(L)$ is the applied voltage, i is the current density, and σ_e^0 and σ_h^0 are the electronic conductivities due to electrons and holes in AgBr in equilibrium with Ag respectively.

Figure 4 shows the plots of i vs. $E(L)$ for the C-type cell at 400 °C. By dividing both sides of Eq. 1 by $\exp(E(L)F/RT) - 1$, we obtain:²⁰⁾

$$\frac{iFL}{RT} \frac{1}{\exp\left(\frac{E(L)F}{RT}\right) - 1} \sigma_e^0 = \exp\left(-\frac{E(L)F}{RT}\right) + \sigma_h^0. \quad (2)$$

From the gradient of the plot of Eq. 2, σ_e^0 can be determined. Similarly, σ_h^0 can be determined from the gradient of the plot of the following equation:²⁰⁾

$$\frac{iFL}{RT} \frac{1}{1 - \exp\left(-\frac{E(L)F}{RT}\right)} = \sigma_e^0 + \sigma_h^0 \exp\left(\frac{E(L)F}{RT}\right). \quad (3)$$

Figure 5 shows the plot of Eq. 2, with a good linear relationship. From the slope of the plot, σ_e^0 was determined. Similarly, σ_h^0 was determined from the plot of Eq. 3.

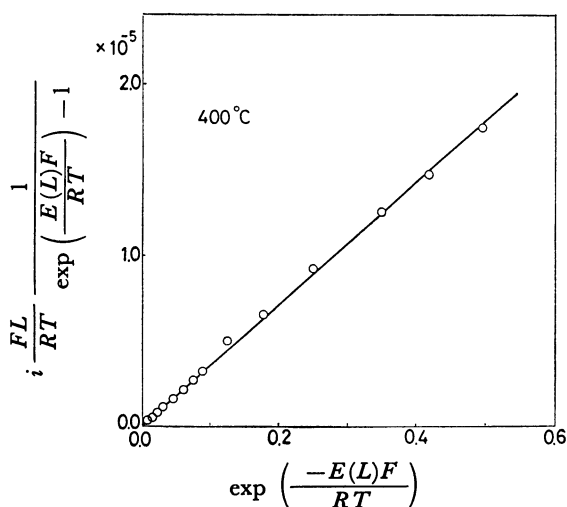


Fig. 5. Plot of $i \frac{FL}{RT} \frac{1}{\exp\left(\frac{E(L)F}{RT}\right) - 1}$ vs. $\exp\left(-\frac{E(L)F}{RT}\right)$ for C-type cell.

According to Mizusaki *et al.*,^{8,10)} we can calculate σ_e and σ_h as functions of the chemical potential of bromine. The results are shown in Fig. 6. The broken line indicates the results obtained by Mizusaki *et al.*⁸⁾ using the A-type cell. The two sets of results are in good agreement, within the limit of experimental error.

The chemical potential profiles under a steady state were also measured for the C-type cell. The results were in good agreement with those obtained by Mizusaki *et al.*⁷⁾ Therefore, it may be concluded that the chemical potential profiles can be well interpreted on the basis

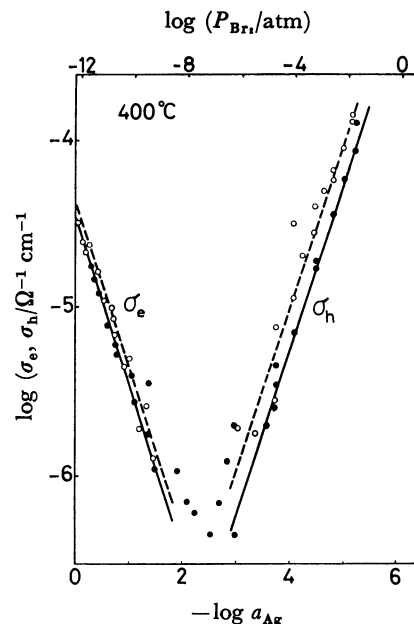


Fig. 6. Plots of σ_e and σ_h vs. $-\log a_{Ag}$ for A and C-type cell.

—: Mizusaki *et al.*⁸⁾ (A-type cell), —: this work (C-type cell).

of Wagner's theory²⁾ and that the same results are obtained under a steady state, whether an A-type cell or a C-type cell is used.

Chemical Diffusion Coefficient. Unlike aqueous electrolyte solutions, solid electrolytes have an electronic conductivity more or less. Therefore, they should be dealt with by the theory on mixed conductors.

According to Ilschner,⁹⁾ silver bromide shows n-type conduction under a low polarization potential and at the temperatures studied. Therefore, the silver bromide can be represented by $Ag_{1+\delta}Br$ ($\delta > 0$). Mizusaki *et al.*⁷⁾ found that δ in silver bromide is distributed linearly under a steady state, as is schematically shown in Fig. 7(a). The distribution of δ is represented by the following equation:

$$\frac{\delta(X) - \delta^0}{\delta(L) - \delta^0} = \frac{X}{L}, \quad (4)$$

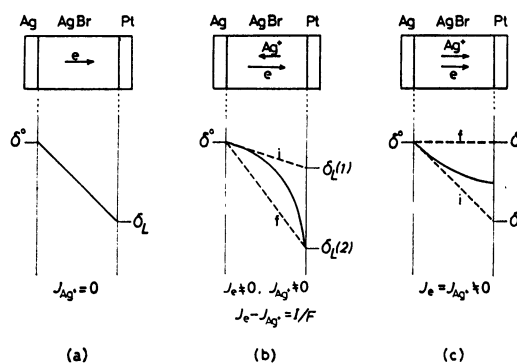


Fig. 7. Schematic diagram of δ profiles.

(a): Steady state, (b): voltage step, (c): open circuit.

i: Initial steady state, t: transient state, f: final steady state.

where $\delta(X)$ denotes δ in Ag_{1+s}Br at the distance, X , from the Ag/AgBr interface, L is the thickness of the silver bromide sample, and δ° is δ in Ag_{1+s}Br equilibrated with Ag .

Voltage-step Method: After the steady state has been attained under the voltage applied, $E_1(L)$, a second voltage, $E_2(L)$, larger than $E_1(L)$ is abruptly applied to the cell. The chemical potential of silver at the AgBr/inert electrode is immediately fixed to that corresponding to $E_2(L)$. The gradient of the electrical field is compensated for quickly by the motion of the major carrier Ag^+ ions, and the electrochemical potential of the Ag^+ ion becomes uniform throughout the silver bromide. The profile of δ in Ag_{1+s}Br changes with the time as is schematically shown in Fig. 7(b). The relaxation process (redistribution of δ) proceeds by means of the counter diffusion of Ag^+ ions and electrons, and the rate is determined exclusively by the diffusion of excess silver atoms. Therefore, the relaxation of δ can be expressed by this equation:

$$\frac{\partial \delta}{\partial t} = \tilde{D} \frac{\partial^2 \delta}{\partial X^2}, \quad (5)$$

where \tilde{D} denotes the chemical diffusion coefficient in n-type AgBr . The chemical diffusion coefficient, \tilde{D} , is determined by solving Eq. 5 analytically with the following boundary conditions:

$$\frac{\delta(X,0) - \delta^\circ}{\delta(L,0) - \delta^\circ} = \frac{X}{L} \quad t = 0, \quad (6)$$

$$\delta(L,t) = \delta^\circ \exp\left(-\frac{E_1(L)F}{RT}\right) \quad t < 0, \quad (7)$$

$$\delta(L,t) = \delta^\circ \exp\left(-\frac{E_2(L)F}{RT}\right) \quad t \geq 0, \quad (8)$$

$$\delta(0,t) = \delta^\circ, \quad (9)$$

where $\delta(X,t)$ denotes the value of δ at a position X apart from the Ag/AgBr interface and at a time t . When t is sufficiently large, the solution of Eq. 5 at $X=L/2$ is:⁹⁾

$$\frac{\delta(L/2,\infty) - \delta(L/2,t)}{\delta(L/2,\infty) - \delta(L/2,0)} = \frac{4}{\pi} \exp\left(-\frac{D\pi^2 t}{L^2}\right). \quad (10)$$

The nonstoichiometry $\delta(X)$ is related to $E(X)$ by means of this equation:

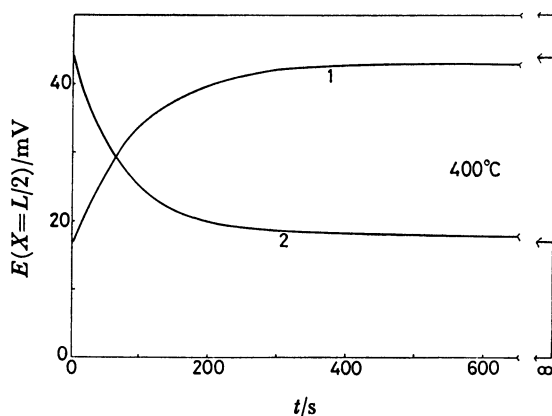


Fig. 8. Time change of $E(L/2)$ for C-type cell.
1: $E(L)$, 40 mV \rightarrow 200 mV, 2: $E(L)$, 200 mV \rightarrow 40 mV.

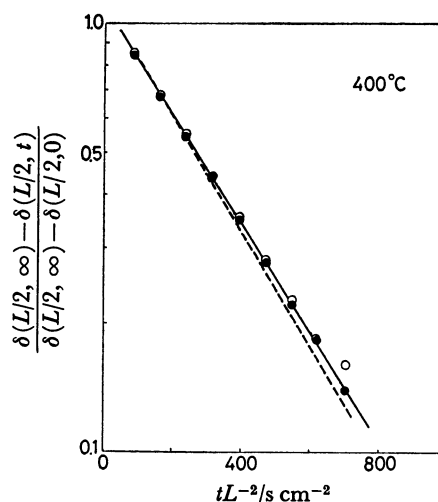


Fig. 9. Plots of $\frac{\delta(L/2,\infty) - \delta(L/2,t)}{\delta(L/2,\infty) - \delta(L/2,0)}$ vs tL^{-2} .

●: $E(L)$, 40 mV \rightarrow 200 mV, ○: $E(L)$, 200 mV \rightarrow 40 mV, —: this work (C-type cell), ----: Mizusaki *et al.*⁹⁾ (A-type cell).

$$\delta(X) = \delta^\circ \exp\left(-\frac{E(X)F}{RT}\right). \quad (11)$$

The time change in $\delta(L/2)$ is calculated from the change in $E(L/2)$.

Figure 8 shows the time change in $E(L/2)$ for the C-type cell. \tilde{D} is determined from the slope of the plot of $\log \{[\delta(L/2,\infty) - \delta(L/2,t)] / [\delta(L/2,\infty) - \delta(L/2,0)]\}$ vs. tL^{-2} . Figure 9 shows the plot. In the figure, the results of the A-type cell are also given. A good agreement is seen between the \tilde{D} values obtained using both types of cells. The results clearly indicate that the IP method gives the same \tilde{D} values, regardless of the nature of the inert electrode.

Open-circuit Method: In the case of the voltage-step method, the electronic current is driven not by the electrical field, but by the concentration gradient of the electrons. The ionic current due to silver ions is not equal to the electronic current ($J_e - J_{\text{Ag}^+} \neq 0$) during the relaxation, as is shown in Fig. 7(b). The difference is observed as the current flowing in the external circuit, and it does not correspond to the flux of mass transport due to the relaxation.

In the case of the OC method, the relaxation proceeds by means of the ambipolar diffusion of silver ions and electrons, because no net current flows in the external circuit. Therefore, the same diffusion situation as in the metal oxidation is set up in this method.

By solving Eq. 5 with the following boundary conditions:

$$\frac{\delta(X,0) - \delta^\circ}{\delta(L,0) - \delta^\circ} = \frac{X}{L} \quad t = 0 \quad (12)$$

$$\frac{\partial(L,t)}{\partial X} = 0 \quad t < 0 \quad (13)$$

$$\delta(0,t) = \delta^\circ \quad t \geq 0 \quad (14)$$

we obtain:

$$\frac{\delta^\circ - \delta(L, t)}{\delta^\circ - \delta(L, 0)} = \frac{8}{\pi^2} \exp\left(\frac{\bar{D}\pi^2 t}{4L^2}\right) \quad (15)$$

for a sufficiently large t . The time change in $\delta(L, t)$ is calculated from $E(L, t)$ by using Eq. 11.

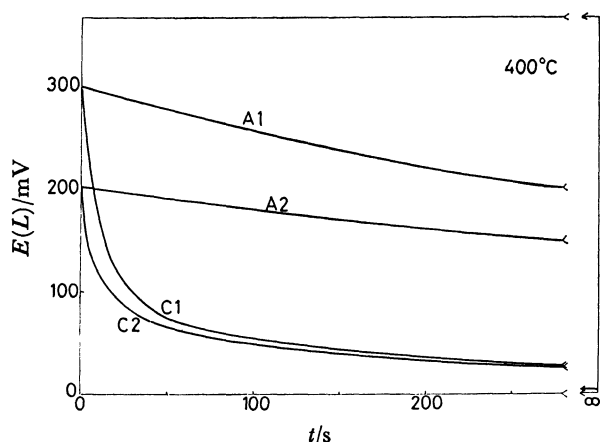


Fig. 10. Time change of $E(L)$ for A and C-type cell. A1: $E(L)=300$ mV (A-type cell), A2: $E(L)=200$ mV (A-type cell), C1: $E(L)=300$ mV (C-type cell), C2: $E(L)=200$ mV (C-type cell).

Accordingly, \bar{D} is determined from the slopes of the plot of $\log [\{\delta^\circ - \delta(L, t)\} / \{\delta^\circ - \delta(L, 0)\}]$ vs. tL^{-2} . Figure 10 shows the time change in the open-circuit voltage $E(L, t)$. As can be seen from the figure, the decay of $E(L, t)$ for the A-type cell is very slow and the reproducibility is poor. On the other hand, the time change in $E(L, t)$ for the C-type cell is reproducible.

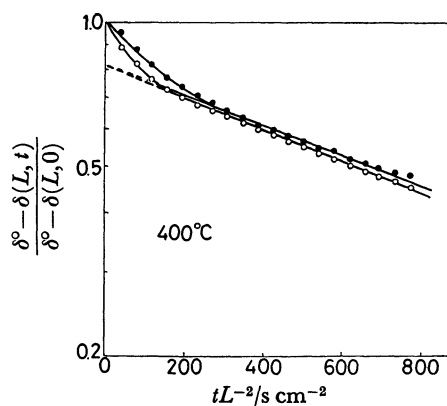


Fig. 11. Plots of $\frac{\delta^\circ - \delta(L, t)}{\delta^\circ - \delta(L, 0)}$ vs. tL^{-2} for C-type cell. \bullet : $E(L, 0)=300$ mV, \circ : $E(L, 0)=200$ mV.

Figure 11 gives the plots for determining \bar{D} . This figure shows that \bar{D} is independent of the voltage applied before opening the circuit. Therefore, \bar{D} in n-type AgBr may be supposed to be independent of δ . From the decay in $E(L, t)$ for the A-type cell, we can not determine the \bar{D} , for the plot of $\log [\{\delta^\circ - \delta(L, t)\} / \{\delta^\circ - \delta(L, 0)\}]$ vs. tL^{-2} is curved.

Figure 12 shows the plots of $\log [\{\delta^\circ - \delta(L, t)\} / \{\delta^\circ - \delta(L, 0)\}]$ vs. tL^{-2} for the C-type cell. As can be seen

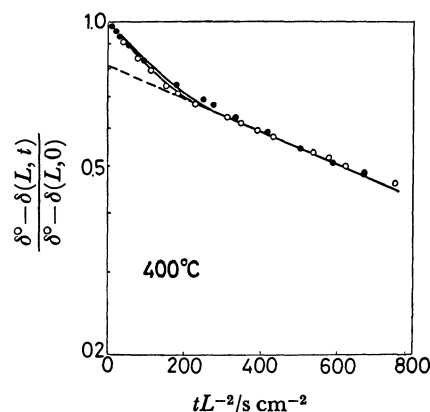


Fig. 12. Plots of $\frac{\delta^\circ - \delta(L, t)}{\delta^\circ - \delta(L, 0)}$ vs. tL^{-2} for C-type cell. \bullet : $L=0.84$ cm, \circ : $L=0.51$ cm.

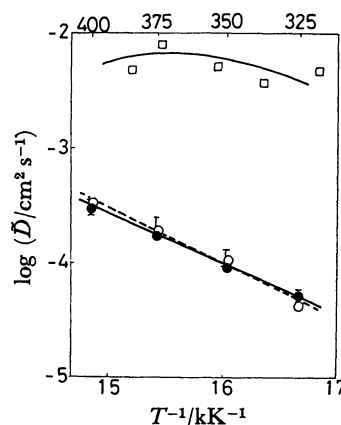


Fig. 13. Arrhenius plots of \bar{D} . \square : B-type cell by Weiss¹⁶⁾ (OC method), \bullet : A-type cell by Mizusaki *et al.*⁹⁾ (IP method), \circ : C-type cell in this work (IP method), \circ : C-type cell in this work (OC method).

from the figure, \bar{D} is independent of the thickness of AgBr. Therefore, it may be concluded that the decay of $E(L, t)$ for the cell is due to the relaxation of δ within AgBr.

Figure 13 gives the Arrhenius plot for \bar{D} of n-type AgBr. The chemical diffusion coefficient, \bar{D} , determined by the IP method using the A and C-type cells and that determined by the OC method using the C-type cell are in good agreement. Therefore, the electronic current driven by the concentration gradient does not affect the mass transfer due to the chemical relaxation. However, \bar{D} can not be determined by the OC method when the A-type cell is used. This may be due to the diffusion and absorption of the Br_2 gas produced by the electrolysis of AgBr in the carbon electrode.

Weiss¹⁶⁾ data obtained by the OC method using the B-type cell is one order of magnitude larger than the other data. In his experiment, the carbon electrode was exposed to an inert atmosphere, and bromine gas was supposed to be liberated at the AgBr/C interface by the electrolysis of AgBr. Therefore, larger \bar{D} values were obtained.

From these results, it seems that the OC method can be used provided that the inert electrode does not absorb or does not react with the electrolysis product. Platinum and gold seem to be appropriate as inert electrodes for the OC method. However, at a high polarization potential (for example, above 777 mV for Ag/AgBr/Pt cell at 400 °C), platinum bromide are produced at the AgBr/Pt interface.²¹ Although gold does not react with bromine at a high polarization potential, the formation of a solid solution with AgBr must be taken into account.

References

- 1) M. H. Hebb, *J. Chem. Phys.*, **20**, 185 (1952).
- 2) C. Wagner, *Proc. C. I. T. C. E.*, **7**, 361 (1955).
- 3) B. Ilschner, *J. Chem. Phys.*, **28**, 1109 (1958).
- 4) D. O. Raleigh, *J. Phys. Chem. Solids*, **26**, 329 (1965).
- 5) Y. I. van der Meulen and F. A. Kröger, *J. Electrochem. Soc.*, **117**, 69 (1970).
- 6) A. V. Joshi and J. B. Wagner, Jr., *J. Electrochem. Soc.*, **122**, 1071 (1975).
- 7) J. Mizusaki, K. Fueki, and T. Mukaibo, *Bull. Chem. Soc. Jpn.*, **48**, 428 (1975).
- 8) J. Mizusaki, K. Fueki, and T. Mukaibo, *Bull. Chem. Soc. Jpn.*, **51**, 692 (1978).
- 9) J. Mizusaki, K. Fueki, and T. Mukaibo, *Bull. Chem. Soc. Jpn.*, **52**, 1890 (1979).
- 10) J. Mizusaki and K. Fueki, *Rev. Chim. Miner.*, **17**, 356 (1980).
- 11) K. Weiss, *Electrochim. Acta*, **16**, 201 (1971).
- 12) A. V. Joshi, "Fast Ion Transport in Solids," ed by W. van Gool, North Holland Publishing Co., (1973), p. 173.
- 13) D. O. Raleigh, *J. Electrochem. Soc.*, **114**, 493 (1967).
- 14) D. O. Raleigh and H. R. Crowe, *J. Electrochem. Soc.*, **116**, 40 (1969).
- 15) J. Goldman and J. B. Wagner, Jr., *J. Electrochem. Soc.*, **121**, 1318 (1974).
- 16) K. Weiss, *Z. Phys. Chem. N. F.*, **59**, 242 (1968).
- 17) J. B. Wagner, Jr., "Electrode Processes on Solid State Ionics," ed by M. Kleitz, Reidel Publ. Co., (1976), p. 185.
- 18) D. O. Raleigh, *J. Phys. Chem.*, **71**, 1785 (1967).
- 19) D. O. Raleigh, "Advances in Electroanalytical Chemistry," Vol. 6, ed by A. J. Bard, M. Dekker, (1973), p. 87.
- 20) J. W. Patterson, E. C. Borgen, and R. A. Rapp, *J. Electrochem. Soc.*, **114**, 752 (1967).
- 21) W. L. Worrell and J. Hladik, "Physics of Electrolytes," ed by J. Hladik, Academic Press, London-New York (1972), p. 747.